Catalysis Today 138 (2008) 97–103

Contents lists available at ScienceDirect

Catalysis Today

journal homepage: www.elsevier.com/locate/cattod

The control of catalytic performance of rutile-type Sn/V/Nb/Sb mixed oxides, catalysts for propane ammoxidation to acrylonitrile

Elena Arcozzi [a], Nicola Ballarini [a], Fabrizio Cavani [a,*], Massimo Cimini [a], Carlo Lucarelli [a], Ferruccio Trifirò [a], Pierre Delichere [b], Jean-Marc M. Millet [b], Philippe Marion [c]

[a] Dipartimento di Chimica Industriale e dei Materiali, Università di Bologna, Viale Risorgimento 4, 40136 Bologna, Italy[1]

[b] Institut de Recherches sur la Catalyse et l'Environnment de Lyon, IRCELYON, UMR5256 CNRS-Université Claude Bernard, Lyon I, 2 avenue A. Einstein, F-69626 Villeurbanne Cedex, France[2]

[c] Rhodia Operations, Centre de Recherches et Technologies, 85, Rue des Frères Perret 69190 Saint Fons, France[2]

ARTICLE INFO

Article history:
Available online 18 June 2008

Keywords:
Propane ammoxidation
Acrylonitrile
Rutile mixed oxides
Tin/vanadium/niobium/antimony mixed oxides

ABSTRACT

This paper describes the effect of the composition of rutile-type Sn/V/Nb/Sb mixed oxides catalysts on the catalytic performance in the gas-phase ammoxidation of propane to acrylonitrile. The variation in the atomic ratio between components in catalysts is the key for the control of activity and selectivity. In samples with atomic composition Sn/V/Nb/Sb 1/0.2/1/x ($0 \leq x \leq 5$) and 1/0.2/y/3 ($0 \leq y \leq 3$) several compounds formed, i.e., SnO_2, Sb/Nb mixed oxide, Sb_6O_{13} and non-stoichiometric rutile-type V/Nb/Sb/O; the latter segregated preferentially at the surface of the catalyst. Tin oxide provided the rutile matrix for the dispersion of the mixed oxides. The main role of Sb was shown to generate mixed oxides containing specific sites for the allylic ammoxidation of propylene intermediately formed. The presence of Nb enhanced the activity and selectivity of these sites.

1. Introduction

One of the most important challenges in the modern chemical industry is the development of new processes allowing the exploitation of alternative raw materials, in replacement of technologies using building blocks derived from oil (olefins and aromatics) and by the way updating the best profitable processes. This has led to research devoted to the valorization of natural gas components, through catalytic, eco-friendly processes of transformation [1]. With that respect, the direct ammoxidation of propane to acrylonitrile is investigated since many years [2–4]. In the current manufacturing process of acrylonitrile by propene ammoxidation, the alkene feedstock cost represents about 67% of the full cost of production. The price differential between propene and propane, which is in average higher than 300 USD/ton, makes competitive a propane ammoxidation process. Asahi Kasei Corporation recently claimed the revamping of an existing 70,000 tons/year acrylonitrile line, for use with propane feedstock.

Two main catalytic systems for the ammoxidation of propane have been described in the literature so far. They are based either on V-antimonates with rutile structure or on multi-component molybdates (Mo/V/Nb/Te/O). The latter, developed by Mitsubishi Kasei [5], gives the highest yield to acrylonitrile, although long-term stability is still unclear. Amongst the antimonates, the preferred catalyst is the Al/Sb/V/W/O system [3,6]. The active phase of this system is a rutile-type mixed oxide containing elements aimed at different roles in the complex transformation of the alkane [7,8]. In regard to this, the rutile structure possesses the flexibility required to accommodate various elements in its framework.

In previous works [9,10], we described a method for the preparation of rutile-type Sn/V/Sb mixed oxides. This method was based on the co-precipitation of the metal oxo-hydrates from an alcoholic solution and its further thermal treatment to develop nano-sized rutile crystallites. Compared to the more crystalline rutile systems prepared with the conventional "slurry" method, the obtained nano-sized rutile crystallites had a greater structural defectivity, a higher specific surface area and hence a higher catalytic activity in propane ammoxidation. In the present work, we report on the variation of the Sb and Nb content in Sn/V/Nb/Sb rutile-type systems to control their catalytic performance in propane ammoxidation.

* Corresponding author.
E-mail address: fabrizio.cavani@unibo.it (F. Cavani).

[1] INSTM, Research Unit of Bologna: a partner of NoE Idecat, FP6 of the EU.

[2] A partner of NoE Idecat, FP6 of the EU.

0920-5861/$ – see front matter © 2008 Elsevier B.V. All rights reserved.
doi:10.1016/j.cattod.2008.04.044

2. Experimental

Catalysts were prepared with the co-precipitation technique, developed for the synthesis of rutile SnO_2-based systems claimed by Rhodia [9]. The preparation consists in dissolving $SnCl_4{\cdot}5H_2O$, $VO(acac)_2$, $SbCl_5$ and $NbCl_5$ in absolute ethanol, and dropping the obtained solution into a buffered aqueous solution maintained at pH 7. The precipitate formed was separated from the supernatant liquid by filtration, dried at 120 °C and finally calcined in air at 700 °C for 3 h.

The XRD patterns of the catalysts were recorded with Ni-filtered Cu Kα radiation (λ = 1.54178 Å) on a Philips X'Pert vertical diffractometer equipped with a pulse height analyzer and a secondary curved graphite-crystal monochromator. Laser-Raman spectra were obtained using a Renishaw 1000 instrument; the samples were excited with the 514 nm Ar line. Specific surface areas were measured using the BET method with nitrogen adsorption (Thermo Instrument). XPS measurements were performed with a VG ESCALAB 200 R. Charging of samples was corrected by setting the binding energy of adventitious carbon (C_{1s}) at 284.5 eV.

Catalytic tests were carried out in a laboratory glass fixed-bed reactor operating at atmospheric pressure. 1.8 g of catalyst was loaded, shaped into particles with size ranging from 0.42 to 0.55 mm. The following reaction conditions were used: feed composition 25 mol% propane, 10% ammonia, 20% oxygen, remainder helium; residence time 2.0 s. The reactor outlet was kept at 170 °C. On-line sampling of a volume of either the feedstock or effluents was obtained by means of three heated valves. Three different columns were used for the products identification. Two of these were a Hay-sep T column (TCD detector) for the separation of CO_2, NH_3, $C_3H_8 + C_3H_6$, H_2O, HCN, acrolein, acetonitrile and acrylonitrile, and a MS-5A column (TCD detector) for separation of O_2, N_2 and CO. Hay-sep T was also used as a filter to avoid the contamination of MS-5A by CO_2. The third column was a packed column filled with Poropak QS (FID detector) used for the separation of propane from propylene.

3. Results and discussion

3.1. Bulk characterization of the catalysts

Samples having composition Sn/V/Nb/Sb = 1/0.2/1/x ($0 \le x \le 5$) and 1/0.2/y/3 ($0 \le y \le 3$) (atomic ratios between components) were prepared. Table 1 reports the theoretical atomic composition, calculated on the basis of the amount of each precursor used for the preparations, the corresponding experimental composition for a few of them (as determined by X-ray Fluorescence) and the values of specific surface areas. The XRF analyses were in good agreement with the theoretical compositions; this was true for both samples having low and high Sb contents and therefore, theoretical compositions were assumed to correspond to the real ones for all the prepared catalysts.

No significant effect of the composition on the surface area was observed; the latter varied between 68 and 79 m^2/g, except for the samples containing the greater amount of Sb (Sn/V/Nb/Sb 1/0.2/1/5, 54 m^2/g) or the greater amount of Nb (Sn/V/Nb/Sb 1/0.2/3/3, 33 m^2/g), or no Nb (Sn/V/Nb/Sb 1/0.2/0/3, 35 m^2/g). It is interesting noting that the surface areas of all catalysts were remarkably higher than the ones typically reported for rutile-type mixed oxides prepared with conventional methods leading to surface areas systematically lower than 10 m^2/g.

Fig. 1 shows the X-ray diffraction patterns of samples with composition Sn/V/Nb/Sb = 1/0.2/1/x, after calcination at 700 °C;

Table 1
Theoretical and experimental (X-ray fluorescence) bulk atomic composition, and specific surface area of the prepared catalysts

Atomic composition (theoretical)	Atomic composition (experimental)	Specific surface area (m^2/g)
Sn/V/Nb/Sb, 1/0.2/1/0	nd	68
Sn/V/Nb/Sb, 1/0.2/1/1	1/0.24/1.25/1.03	79
Sn/V/Nb/Sb, 1/0.2/1/2	nd	79
Sn/V/Nb/Sb, 1/0.2/1/3	1/0.20/1.16/2.81	74
Sn/V/Nb/Sb, 1/0.2/1/4	nd	70
Sn/V/Nb/Sb, 1/0.2/1/5	1/0.20/1.11/4.79	54
Sn/V/Nb/Sb, 1/0.2/0/3	nd	35
Sn/V/Nb/Sb, 1/0.2/1/3	1/0.20/1.16/2.81	74
Sn/V/Nb/Sb, 1/0.2/2/3	nd	69
Sn/V/Nb/Sb, 1/0.2/3/3	nd	33

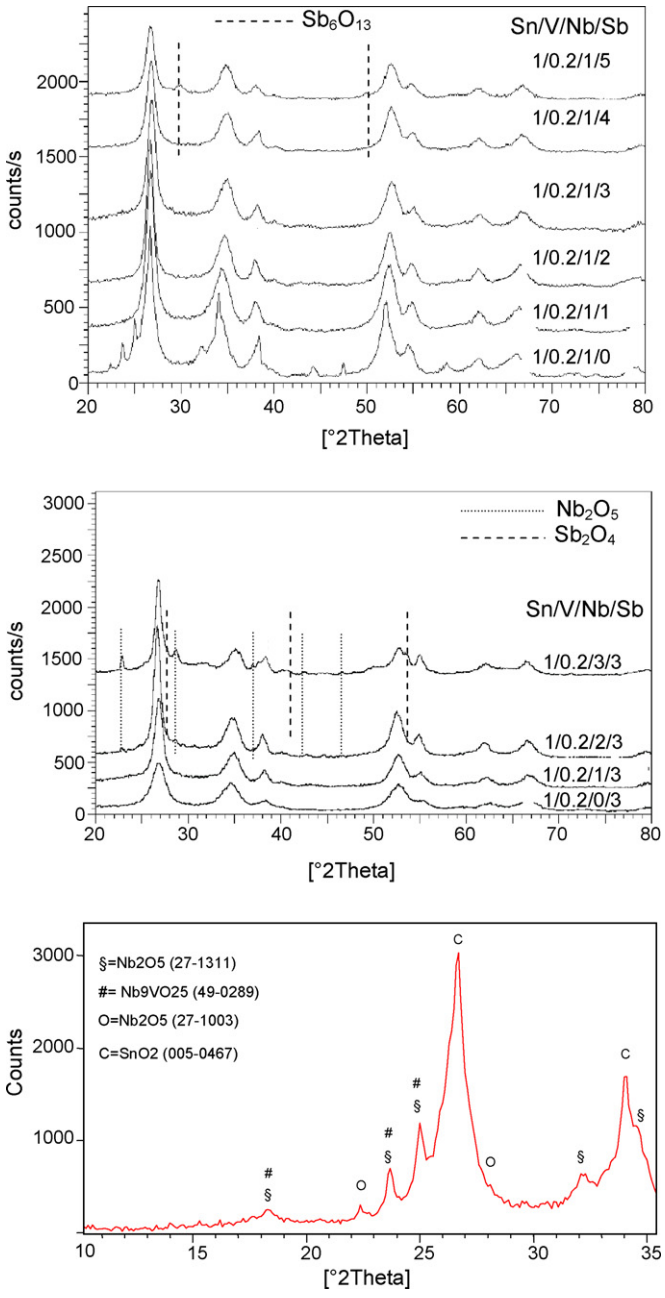

Fig. 1. XRD patterns of calcined Sn/V/Nb/Sb 1/0.2/1/x (top) and 1/0.2/y/3 (middle) (atomic ratios) samples. Bottom: details of the pattern of sample Sn/V/Nb/Sb 1/0.2/1/0.

the bottom figure details the pattern of the Sn/V/Nb/Sb 1/0.2/1/0 sample in the 10–35° 2θ range. All patterns showed the reflections typical of rutile SnO_2 cassiterite (JPCDS file 005-0467) with crystallite size lower than 10 nm. Additional reflections detected in the pattern of the sample without Sb ($x = 0$) belong to monoclinic Nb_2O_5 and orthorhombic Nb_2O_5 (27–1311 and 27–1003, respectively). The presence in this compound of a Nb-rich V/Nb mixed oxide cannot be excluded (VNb_9O_{25}, 49-0289). It can be noted that despite the relevant amount of Sb, most of it was present in the catalysts under the form of an amorphous oxide phase. Only in the case of the sample with the highest Sb content ($x = 5$), some very weak reflections attributed to Sb_6O_{13} were observed.

Before discussing the Raman spectra of samples Sn/V/Nb/Sb 1/0.2/1/x (reported in Fig. 2), it is worth reminding the typical Raman features of reference single and binary oxides. Tin oxide, when prepared with the same precipitation procedure adopted for multi-component samples, has a strong Raman band at 625–630 cm^{-1} and weaker ones at 770 and 685 cm^{-1}, all corresponding to bulk vibration modes. The Raman spectrum of hydrated Nb oxide, when calcined at temperatures between 500 and 700 °C, shows a broad band at 680–690 cm^{-1} and less intense bands at 140, 220 and 310 cm^{-1}. The thermal treatment of Nb oxide at temperatures higher than 700 °C yields a completely different spectrum, with a strong band at 1000 cm^{-1}, assigned to terminal niobyl species, two intense bands between 700 and 800 cm^{-1} and one below 300 cm^{-1} [11–13]. After calcination at above 900 °C, the monoclinic form of niobium oxide (H–Nb_2O_5) shows bands at 992, 674, 623, 261 and 236 cm^{-1} [12,13]. The Raman spectrum of rutile $VNbO_4$ has bands at 990, 920 and 620 cm^{-1} [14,15]; however, this compound is stable at temperatures higher than 500 °C only under O_2-free atmosphere. Nb-rich V/Nb mixed oxides, e.g., VNb_9O_{25} or $V_4Nb_{18}O_{55}$, are obtained by thermal decomposition in air at 700 °C of orthorhombic $VNbO_5$ [14,15]. The Raman spectrum of a reference Sn/Sb/O compound prepared by calcination of a Sn/Sb 1/1 precipitate has two strong Raman bands at 640 and 450 cm^{-1}. The spectrum of $SbNbO_4$ exhibits bands at 845, 685, 620 and 380 cm^{-1} [16,17].

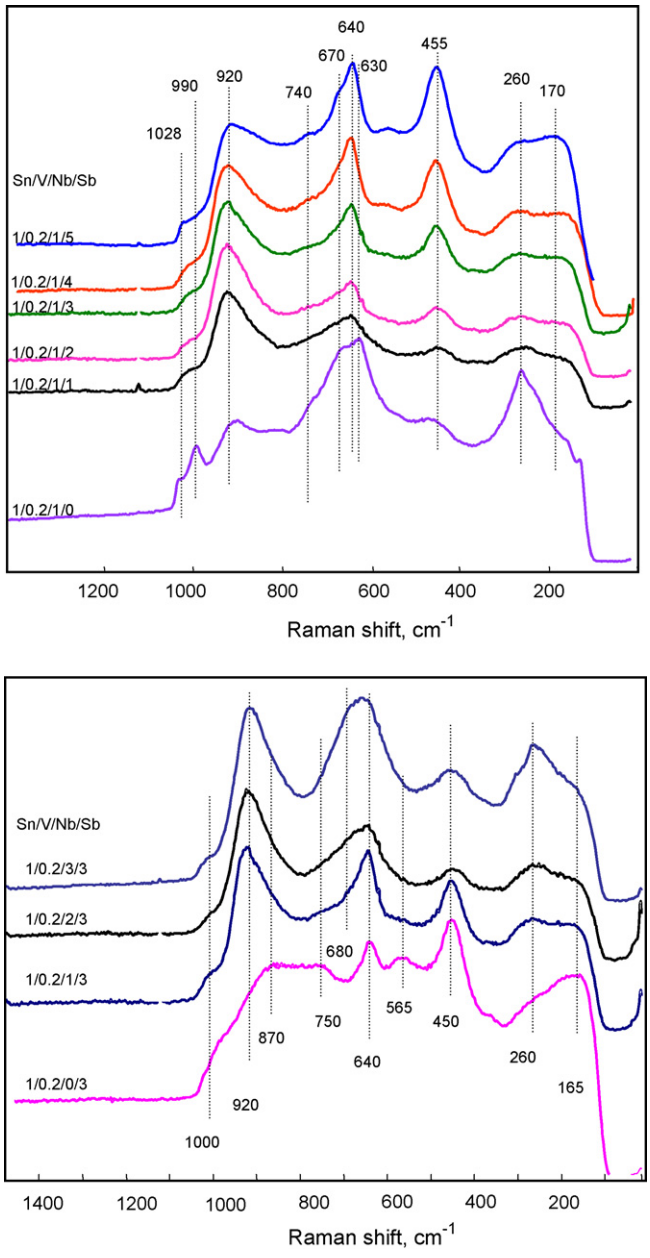

Fig. 2. Raman spectra of calcined Sn/V/Nb/Sb 1/0.2/1/x (top) and 1/0.2/y/3 (bottom) (atomic ratios) samples.

In the Raman spectrum of sample Sn/V/Nb/Sb 1/0.2/1/0, the band at 630 cm^{-1} can be assigned to SnO_2, whereas bands at 990, 670, 260 and 240 cm^{-1} are attributed to monoclinic H–Nb_2O_5 [12,13]. When Sb was added ($x > 0$), the band at 630 cm^{-1} disappeared whereas a new one appeared at 640 cm^{-1}, which can be attributed to the incorporation of Sb^{5+} into the tin oxide [18]. The intensity of the bands attributed to Nb_2O_5 decreased and the formation of a rutile-type V/Nb/Sb mixed oxide likely occurred [19]. When $x > 2$, the increase of intensity of the band at 455 cm^{-1} can be related to the formation of Sb_6O_{13}; however, the 100% intensity band of Sb_6O_{13} should fall at 470 cm^{-1}. This relevant shift can be attributed to the dissolution of guest cations, e.g., Sn^{4+} or Nb^{5+} ions, inside the Sb oxide lattice.

One peculiarity of the mixed oxides prepared with the co-precipitation technique is the high concentration of structural cationic vacancies [19]. In rutile-type systems, e.g., in quasi-$VSbO_4$, mixed Fe/V/Sb/O and Mo/V/Sb/O, such vacancies are formed either because of the excess positive charges generated by oxidation of V^{3+} to V^{4+} and V^{5+}, or of the incorporation of altervalent cations [6,7,20]. The strong intensity of the band at 920 cm^{-1} in the Sn/V/Nb/Sb/O samples is an indication of the high concentration of cationic vacancies.

X-ray diffraction patterns and Raman spectra of samples with composition Sn/V/Nb/Sb 1/0.2/y/3 are reported in Figs. 1 and 2, respectively. The XRD patterns show the presence of only a rutile-type structure except that for the sample with the higher Nb content ($y = 3$) showing additionally the orthorhombic form of Nb_2O_5. The Raman spectrum of sample Sn/V/Nb/Sb 1/0.2/0/3 ($y = 0$) shows the bands of quasi-$VSbO_4$ [6], with additional bands attributable to Sn/Sb/O at 640 cm^{-1} and Sb_6O_{13} at 455 cm^{-1}. The presence of Nb ($y = 1, 2$) led to a decrease of the intensity for the latter band and to the concomitant strong increase of that attributed to cationic vacancies (920 cm^{-1}). This suggests that the addition of Nb forced Sb to form non-stoichiometric mixed oxides, rather than dispersed Sb oxide. An analogous behavior was observed in the case of Cr/V/Nb/Sb systems [19], with the development of a mixed Cr/V antimonate/niobate and of a Sb/Nb mixed oxide to the depends of antimony oxide for Nb-containing samples.

In samples having the highest Nb contents ($y = 2, 3$), bands at 670–680 cm^{-1} and 250–260 cm^{-1} are attributed to orthorhombic Nb_2O_5 [11–13], which is in agreement with XRD results.

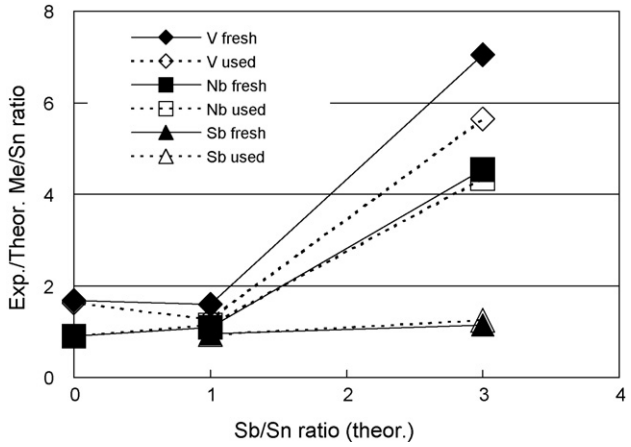

Fig. 3. Experimental/theoretical Me/Sn atomic ratio (Me = V, Nb, Sb) as a function of the theoretical Sb/Sn ratio.

3.2. Surface characterization of the catalysts

Fig. 3 compares the experimental (XPS)-to-theoretical surface Me/Sn ratio (Me = V, Nb, Sb) in the samples having composition Sn/V/Nb/Sb 1/0.2/1/*x*; the abscissa (the theoretical Sb/Sn atomic ratio) corresponds to the *x*-value in the compositions. The greater the exp/theor Me/Sn ratio, the greater the deviation from the theoretical bulk ratio is; this deviation corresponds to a surface enrichment of Me with respect to the expected amount. The calculated values are reported for both fresh (calcined) and spent samples (catalysts downloaded after reactivity tests). The binding energy values indicate the presence of V^{3+} (V $2p_{3/2}$ 515.9–516.2 eV) and V^{4+} (V $2p_{3/2}$ 517.2–517.4 eV; however, the presence of V^{5+} cannot be excluded), of Nb^{5+}(Nb $3d_{5/2}$ 207.1–207.2 eV), Sn^{4+} (Sn $3d_{5/2}$ 486.9–487.1 eV) and Sb^{5+} (Sb $3d_{3/2}$ 540.4–540.5 eV). The absence of the signal of Sb^{3+} may be attributed either to the presence of a low amount of Sb_6O_{13}, or to a modification of this oxide because of the incorporation of altervalent cations, e.g., Sn^{4+}.

Both in fresh and in used samples, XPS data clearly show that surface V/Sn ratio was close to the theoretical (bulk) ratio in samples with *x* = 0 (Sb/Sn = 0) and *x* = 1 (Sb/Sn = 1); in fact, the exp/theor V/Sn ratio was close to 1.5, indicating a rather homogeneous dispersion of the two elements in the samples. On the contrary, in the case of the sample with *x* = 3 (Sb/Sn = 3), a surface segregation of V occurred, as evidenced by the very high exp/theor V/Sn ratio. The same occurred for Nb; the exp/theor Nb/Sn ratio was close to 1 in samples with *x* = 0 and 1, while it was equal to 4.5 in the sample with *x* = 3. The XPS data also show that the experimental surface Sb/Sn ratio in samples with *x* = 1 and 3 was the same as the theoretical bulk ratio. The two elements were therefore reciprocally uniformly dispersed for the range of composition examined. No tremendous change was observed in the surface atomic composition of the used samples as compared to the fresh ones. Only the sample with *x* = 3 (Sb/Sn = 3) showed a higher surface enrichment in V before catalytic test (exp/theor V/Sn ratio = 7) than after (exp/theor V/Sn ratio = 5.5).

3.3. The nature of Sn/V/Nb/Sb mixed oxides

The structural (XRD, Raman spectroscopy) and surface (XPS) characterization led together to the following conclusions:

1. In the sample of composition Sn/V/Nb/Sb 1/0.2/1/0, the main components were SnO_2 cassiterite and Nb_2O_5. Vanadium likely formed a V/Nb mixed oxide, but also in part dissolved in the cassiterite lattice [21]. There was no preferential segregation of any component at the particle surface.
2. The addition of Sb in an amount comparable to that of Nb and Sn (*x* = 1) in Sn/V/Nb/Sb 1/0.2/1/*x*, did not lead to relevant modifications in the dispersion of elements; however, both SnO_2 and Nb_2O_5 were no longer present, due to the formation of a Sn/Sb mixed oxide and of a non-stoichiometric rutile-type V/Sb/Nb mixed oxide, corresponding to either a $VNb_zSb_{1-z}O_4$ [19] or a $SbNb_{1-z}V_zO_4$ [22] solid solution. In the former case the oxide is a mixed niobate/antimonate containing only Sb^{5+}, whereas in the latter case it is a mixed niobate/vanadate containing both Sb^{3+} and Sb^{5+}. In this last case, Sb^{5+} is formed by oxidation of Sb^{3+} (the species in stoichiometric $SbNbO_4$) to balance the electronic charges because of the replacement of V^{4+} for Nb^{5+}. The remarkable increase of cationic vacancies in Nb-containing samples as compared to the Sn/V/Sb/O catalyst can be attributed to the substitution of V^{3+} or V^{4+} by Nb^{5+}.
3. In samples containing higher amount of Sb (*x* > 1), Sb and Sn remained reciprocally dispersed; also small amount of Sb_6O_{13} formed. A partial dissolution of other type of cations (i.e., Sn^{4+}, Nb^{5+}) in Sb_6O_{13} is also likely. The defective V/Sb/Nb mixed oxide segregated at the catalyst surface.
4. In the case of samples in which the amount of Sb was fixed and that of Nb was varied (Sn/V/Nb/Sb 1/0.2/*y*/3), when *y* = 0 the catalyst contained, besides Sb_6O_{13}, rutile quasi-$VSbO_4$ and SnO_2 also incorporating Sb^{5+}. The addition of Nb (*y* = 1) caused the decrease of the amount of Sb oxide, and the incorporation of Nb to form defective, rutile-type V/Sb/Nb mixed oxide. In samples with *y* = 2 and 3, Nb_2O_5 was also detected.

3.4. Catalytic properties: samples Sn/V/Nb/Sb 1/0.2/1/x

The catalytic performance of samples Sn/V/Nb/Sb 1/0.2/1/*x* is summarized in Figs. 4 and 5 showing respectively, the conversion of propane and the selectivity to acrylonitrile as a function of the reaction temperature for the different catalysts. The progressive increase of Sb content led to a considerable decrease of catalytic activity; sample with *x* = 0 gave 22% propane conversion and total oxygen conversion at 430 °C, while the catalyst with *x* = 3 reached the same conversion at 530 °C. However, the former catalyst was quite unselective to acrylonitrile and the main products were propylene, carbon oxides and acetonitrile.

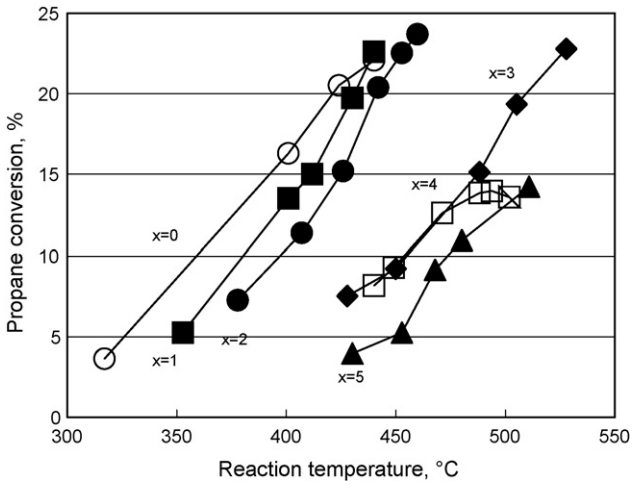

Fig. 4. Effect of reaction temperature on propane conversion, for catalysts with composition Sn/V/Nb/Sb = 1/0.2/1/*x*.

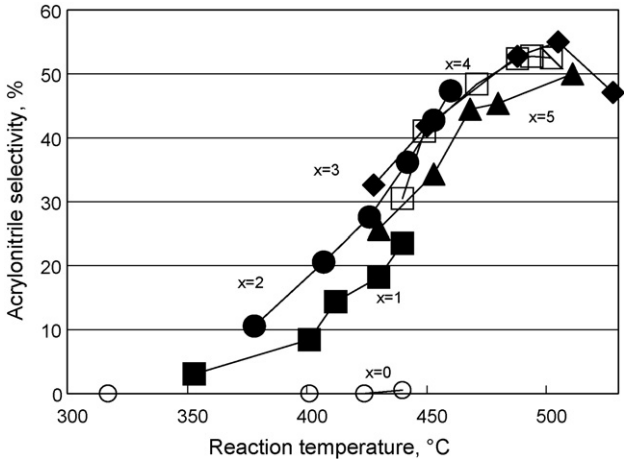

Fig. 5. Effect of reaction temperature on selectivity to acrylonitrile, for catalysts with composition Sn/V/Nb/Sb = 1/0.2/1/*x*.

The lower activity of Sb-containing catalysts, as compared to the Sb-free sample, was not due to lower surface areas (see Table 1). The phase characterization of catalysts evidenced that in the latter catalyst vanadium likely formed a V/Nb mixed oxide. This compound has catalytic sites active and fairly selective for the first reaction step, i.e., the propane oxidative dehydrogenation to propylene [14], but no efficient sites for the last one, i.e., the allylic ammoxidation [23]. The addition of Sb (samples with $x = 1$, 2) favored the formation of a rutile-type V/Sb/Nb mixed oxide; V/Sb/O has both sites active in propane oxidative dehydrogenation [24], and sites selective for the ammoxidation reaction [19]. The increase of selectivity to acrylonitrile with temperature and the concomitant decrease of selectivity to propylene (Fig. 6) were due to the fact that higher temperatures favor the ammoxidation to acrylonitrile of the olefin intermediately formed.

Fig. 5 shows that samples Sn/V/Nb/Sb 1/0.2/1/*x* having $x = 0$–2 were less selective to acrylonitrile than those having $x > 2$; with all catalysts, the highest selectivity was obtained in correspondence of the highest propane conversion, the latter having been reached when the limiting reactant conversion was total.

Samples having $x = 3$–5 yielded 15% propane conversion at approximately 500 °C; this allows a comparison of the selectivity to acrylonitrile for similar temperatures and conversions. The maximum selectivity shown by the sample of composition Sn/V/Nb/Sb 1/0.2/1/3 ($x = 3$) was 55%, slightly higher than the selectivity of the sample with $x = 4$ (52%) and of that with $x = 5$ (50%).

However, the greater improvement of selectivity to acrylonitrile was observed when the Sb content was increased from $x = 0$ to $x = 1$ and 2. It is reported in the literature that in order to be selective in propane ammoxidation, a V/Sb/O catalyst should have free, amorphous antimony oxide dispersed over the rutile $VSbO_4$ [4]; in fact, antimony oxide contains the Sb–O–Sb sites that in the presence of gas-phase ammonia are transformed into active Sb–(NH)–Sb species. These sites would perform the $(NH)^{2-}$ insertion onto the allylic intermediate. Only when the Sb/V atomic ratio is much higher than 1, i.e., optimally higher than 3 but lower than 6–7, the right combination of sites activating the alkane (V^{4+} in rutile-type phase) and of selective sites (Sb–O–Sb mostly in antimony oxide) is achieved, giving the highest yield and selectivity to acrylonitrile. In our samples, Sb was in excess with respect to V even in the sample with $x = 1$. However, a part of Sb was incorporated in the Sn/Sb and rutile V/Nb/Sb mixed oxides phases; this feature is related to the total composition of the samples including the presence of Nb. Therefore, the best selectivity to acrylonitrile was finally obtained with samples having $x > 1$.

Fig. 7 reports the distribution of the reaction products for the catalysts investigated, obtained in correspondence with the highest acrylonitrile yield. The catalyst without Sb ($x = 0$) gave CO and CO_2 as main products; the increase of the Sb content caused the progressive decline of the selectivity to CO_x (especially CO) and to propylene, and the increase of the selectivity to HCN and acrylonitrile.

3.5. Catalytic properties: samples Sn/V/Nb/Sb 1/0.2/*y*/3

Figs. 8–10 report the results of catalytic testing with samples Sn/V/Nb/Sb 1/0.2/*y*/3. The conversion for catalysts with $y = 0$ and 1 was similar, despite the higher surface area of the Nb-containing sample. Therefore, the presence of Nb decreased the catalyst activity, possibly because of the partial substitution of V^{4+} in rutile by Nb^{5+}. Both samples gave total conversion of oxygen at approximately 530 °C (Fig. 8); however, in the former case the selectivity to acrylonitrile decreased considerably more when the temperature was increased from 500 to 530 °C. Catalysts having the higher amount of Nb ($y = 2$ and 3) were more active; both gave total oxygen conversion at 480–490 °C. However, the selectivity to acrylonitrile was lower than that obtained with the catalyst having

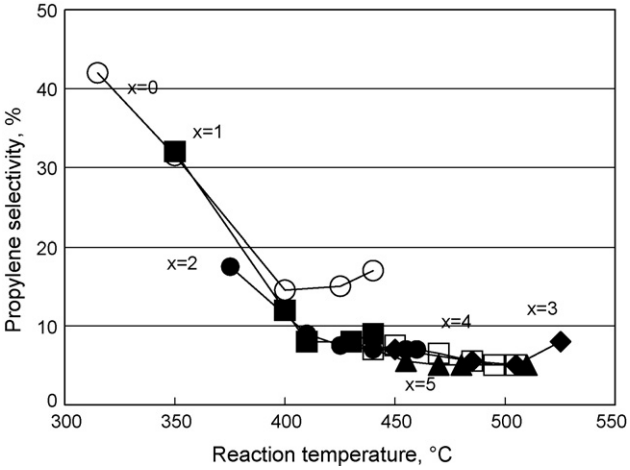

Fig. 6. Effect of reaction temperature on selectivity to propylene, for catalysts with composition Sn/V/Nb/Sb = 1/0.2/1/*x*.

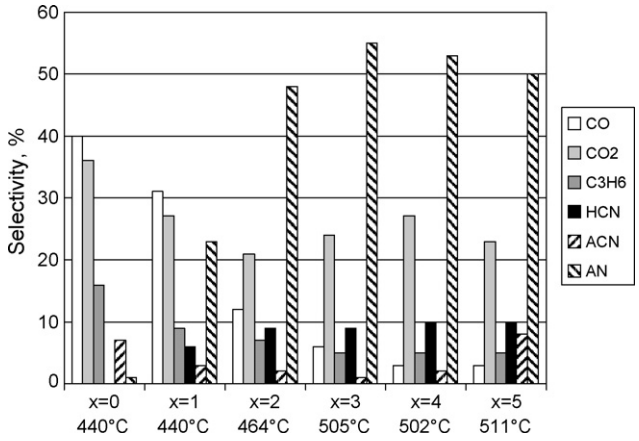

Fig. 7. Selectivity to the reaction products at the temperature at which the acrylonitrile yield is the highest, for catalysts with composition Sn/V/Nb/Sb = 1/0.2/1/*x*. HCN: cyanhydric acid; ACN: acetonitrile; AN: acrylonitrile.

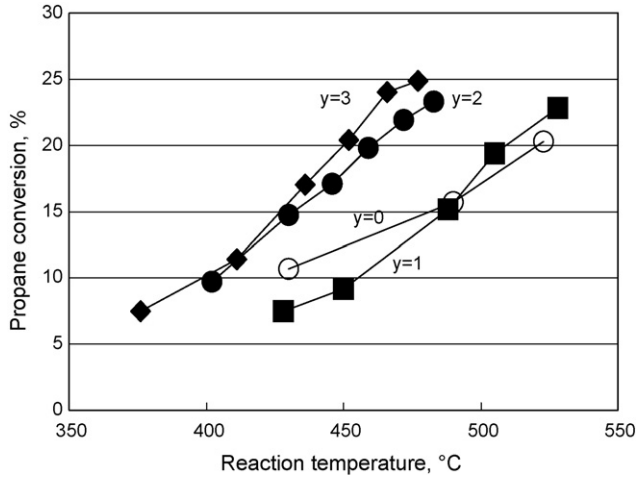

Fig. 8. Effect of reaction temperature on propane conversion, for catalysts with composition Sn/V/Nb/Sb = 1/0.2/*y*/3.

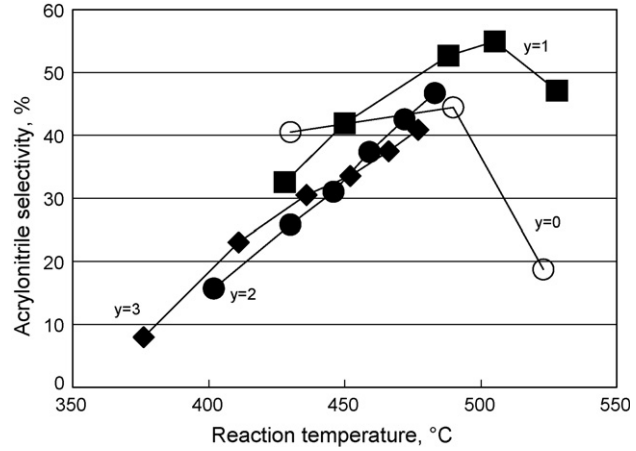

Fig. 9. Effect of reaction temperature on selectivity to acrylonitrile, for catalysts with composition Sn/V/Nb/Sb = 1/0.2/*y*/3.

y = 1. With these catalysts, also Nb_2O_5 likely contributed to the non-selective activation of the alkane.

Fig. 10 shows the distribution of products, obtained at the highest acrylonitrile yield. The addition of Nb led to an increase of the selectivity to CO, propylene and acetonitrile, and to a relevant decrease of the selectivity to CO_2; the formation of HCN was not affected by Nb. The selectivity to acrylonitrile reached a maximum for an intermediate Nb content (*y* = 1). Therefore, as long as Nb was present in relatively low amount, it improved the selectivity of sites aimed at allylic ammoxidation. At higher Nb content, the selectivity to acrylonitrile decreased mainly to the benefit of that to CO. This lower efficiency could be due to the presence of the crystalline Nb_2O_5 phase.

The incorporation of Nb^{5+} in the rutile lattice, and eventually also in free antimony oxide, may affect the allylic ammoxidation properties of Sb–O–Sb sites, either through an enhanced rate of formation of the Sb–(NH)–Sb active species, or through an enhanced ability for transferring the imino species onto the allylic intermediate. This might occur because of the formation of a Nb–O–Sb active site. An alternative explanation for the positive effect of Nb on selectivity to acrylonitrile is the generation of cationic vacancies in the rutile V/Nb/Sb mixed oxide [6,7,20]. Raman spectroscopy showed that the addition of either Nb to Sn/V/Sb/O or Sb to Sn/V/Nb/O, led to the development of a rutile-type V/Nb/Sb mixed oxide, more defective than the corresponding V/Sb mixed oxide in the Sn/V/Sb/O sample and the V/Nb mixed oxide in the Sn/V/Nb/O sample. An analogous effect was observed in rutile-type Cr/V/Nb/Sb mixed oxides [19], in which a progressive increase of the Sb content caused an increase of the concentration of cationic vacancies, with an improvement of the selectivity to acrylonitrile.

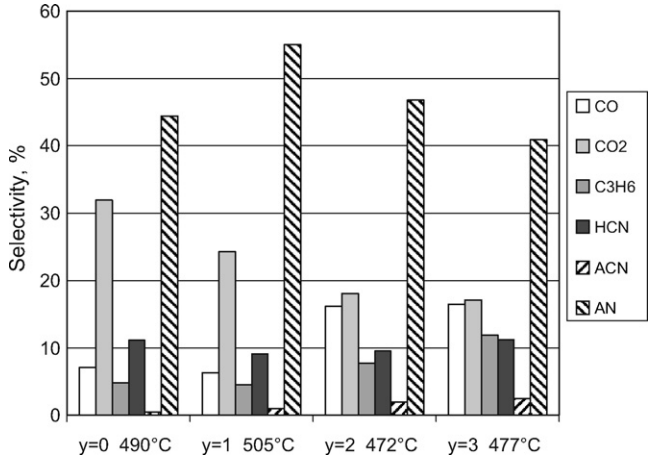

Fig. 10. Selectivity to the reaction products at the temperature at which the acrylonitrile yield is the highest, for catalysts with composition Sn/V/Nb/Sb = 1/0.2/*y*/3. HCN: cyanhydric acid; ACN: acetonitrile; AN: acrylonitrile.

4. Conclusions

Sn/V/Nb/Sb/O are efficient catalysts for the ammoxidation of propane to acrylonitrile under hydrocarbon-rich conditions. The catalysts, when prepared by co-precipitation from an alcoholic medium, consist of nano-sized crystals of dispersed mixed oxides, with specific surface area ranging between 60 and 70 $m^2\ g^{-1}$. Tin oxide incorporates Sb cations, and provides the rutile matrix for the dispersion of the active components.

Antimony and niobium have two opposite effects on activity, but similar effects on selectivity to acrylonitrile. Antimony is necessary for the generation of sites aimed at transforming intermediate propylene to acrylonitrile; the sample without Sb (Sn/V/Nb/Sb 1/0.2/1/0) does not produce acrylonitrile. The formation of the defective rutile-type V/Sb/Nb mixed oxide in the sample containing both Sb and Nb (Sn/V/Nb/Sb 1/0.2/1/1) is the reason for the increase of the selectivity to acrylonitrile. The efficiency in acrylonitrile formation is the greater in samples containing excess Sb, i.e., with composition Sn/V/Nb/Sb 1/0.2/1/3, although the catalytic activity decreases with Sb addition.

The catalyst without Nb (Sn/V/Nb/Sb 1/0.2/0/3) is active and selective in propane ammoxidation; however, the presence of Nb (Sn/V/Nb/Sb 1/0.2/1/3) improves both the activity and the selectivity to acrylonitrile. This effect is attributed to the incorporation of Nb in the rutile-type phase. However, when a large amount of Nb is present (Sn/V/Nb/Sb 1/0.2/2/3 and 1/0.2/3/3), the presence of Nb_2O_5 decreases the selectivity to acrylonitrile.

Acknowledgement

Rhodia is acknowledged for financial support.

References

[1] P. Arpentinier, F. Cavani, F. Trifirò, The Technology of Catalytic Oxidations, Editions Technip, Paris, 2001.
[2] F. Cavani, F. Trifirò, in: M. Baerns (Ed.), Basic Principles in Applied Catalysis, Series in Chemical Physics 75, Springer, Berlin, 2003, p. 21.
[3] R.K. Grasselli, Topics Catal. 21 (2002) 79.

[4] G. Centi, S. Perathoner, F. Trifiro, Appl. Catal. A 157 (1997) 143.
[5] T. Ushikubo, K. Oshima, A. Kayou, M. Vaarkamp, M. Hatano, J. Catal. 169 (1997) 394.
[6] J. Nilsson, A.R. Landa-Canovas, S. Hansen, A. Andersson, J. Catal. 186 (1999) 442.
[7] H. Roussel, B. Mehlomakulu, F. Belhadj, E. Van Steen, J.M.M. Millet, J. Catal. 205 (2002) 97.
[8] V.D. Sokolovskii, A.A. Davydov, O.Yu. Ovsitser, Catal. Rev. -Sci. Eng. 37 (3) (1995) 425.
[9] G. Blanchard, P. Burattin, F. Cavani, S. Masetti, F. Trifirò, WO Patent 97/23,287 A1 (1997), assigned to Rhodia.
[10] S. Albonetti, G. Blanchard, P. Burattin, F. Cavani, S. Masetti, F. Trifirò, Catal. Today 42 (1998) 283.
[11] J.-M. Jehng, I.E. Wachs, Chem. Mater. 3 (1991) 100.
[12] R. Brayner, F.B. Verduraz, Phys. Chem. Chem. Phys. 5 (2003) 1457.
[13] B.X. Huang, K. Wang, J.S. Church, Y.-S. Li, Electron. Acta 44 (1999) 2571.
[14] N. Ballarini, F. Cavani, C. Cortelli, C. Giunchi, P. Nobili, F. Trifirò, R. Catani, U. Cornaro, Catal. Today 78 (2003) 353.
[15] N. Ballarini, G. Calestani, R. Catani, F. Cavani, U. Cornaro, C. Cortelli, M. Ferrari, Stud. Surf. Sci. Catal. 155 (2005) 81.
[16] M.O. Guerrero-Perez, J.L.G. Fierro, M.A. Bañares, Catal. Today 78 (2003) 387.
[17] M.O. Guerrero-Perez, J.L.G. Fierro, M.A. Bañares, Phys. Chem. Chem. Phys. 5 (2003) 4032.
[18] M. Caldararu, M.F. Thomas, J. Bland, D. Spranceana, Appl. Catal. A 209 (2001) 383.
[19] N. Ballarini, F. Cavani, M. Cimini, F. Trifirò, J.M.M. Millet, U. Cornaro, R. Catani, J. Catal. 241 (2006) 255.
[20] M. Cimini, J.M.M. Millet, F. Cavani, J. Solid State Chem. 177 (2004) 1045.
[21] F. Cavani, F. Trifirò, A. Bartolini, D. Ghisletti, M. Nalli, A. Santucci, J. Chem. Soc., Faraday Trans. 92 (1996) 4321.
[22] Y. Mimura, K. Ohyachi, I. Matsuura, Science and Technology in Catalysis 1998, Kodansha, Tokyo, 1999, p. 69.
[23] F. Cavani, N. Ballarini, M. Cimini, F. Trifirò, M. Bañares, M.O. Guerrero-Perez, Catal. Today 112 (2006) 12.
[24] V. Cortes Corberan, V.V. Savkin, P. Ruiz, V.P. Vislovskii, J. Mol. Catal. A 158 (2000) 271.